Threefold Increase of the Bulk Electron Temperature of Plasma Discharges in a Magnetic Mirror Device

P. A. Bagryansky,[1,2,*] A. G. Shalashov,[1,3,4,†] E. D. Gospodchikov,[1,3,4] A. A. Lizunov,[1] V. V. Maximov,[1,2] V. V. Prikhodko,[1,2] E. I. Soldatkina,[1,2] A. L. Solomakhin,[1,2] and D. V. Yakovlev[2]
[1]*Budker Institute of Nuclear Physics, 11 Lavrentieva ave., 630090 Novosibirsk, Russia*
[2]*Novosibirsk State University, 2 Pirogova str., 630090 Novosibirsk, Russia*
[3]*Institute of Applied Physics, Russian Academy of Sciences, 46 Ulyanova str., 603950 Nizhny Novgorod, Russia*
[4]*Lobachevsky State University of Nizhny Novgorod, 23 Gagarina ave., 603950 N. Novgorod, Russia*
(Received 18 November 2014; published 18 May 2015)

This Letter describes plasma discharges with a high temperature of bulk electrons in the axially symmetric high-mirror-ratio ($R = 35$) open magnetic system gas dynamic trap (GDT) in the Budker Institute (Novosibirsk). According to Thomson scattering measurements, the on-axis electron temperature averaged over a number of sequential shots is 660 ± 50 eV with the plasma density being $0.7 \times 10^{19}\ \mathrm{m}^{-3}$; in few shots, electron temperature exceeds 900 eV. This corresponds to at least a threefold increase with respect to previous experiments both at GDT and at other comparable machines, thus, demonstrating the highest quasistationary (about 1 ms) electron temperature achieved in open traps. The breakthrough is made possible by application of a new 0.7 MW/54.5 GHz electron cyclotron resonance heating system in addition to standard 5 MW heating by neutral beams, and application of a radial electric field to mitigate the flute instability.

DOI: 10.1103/PhysRevLett.114.205001 PACS numbers: 52.55.Jd, 52.50.Gj, 52.50.Sw

Open magnetic systems for plasma confinement have a number of potential advantages for fusion reactors with various thermonuclear applications starting from neutron sources with a thermonuclear gain factor $Q < 1$ [1,2] and ending with power plants with $Q \gg 1$ [3,4]. In addition to the simplicity of their design, the advantages of open systems are inherent steady-state operation, proven capability of high-β plasma confinement (β is the ratio of the plasma pressure to the magnetic field pressure), no disruptions because there is no plasma current, a relatively low wall loading by plasma heat and radiation, natural diverters with a large area to absorb power, and the possibility of directly converting plasma "exhaust" to electricity. Axisymmetric magnetic mirrors provide additional advantages: no neoclassical radial transport, high field magnets enable simple tandem mirror power plants [5], maintenance and upgrades are easier, and thick-liquid walls become feasible, reducing or eliminating issues of neutron damage to materials. Alternative magnetohydrodynamic (MHD) stabilization techniques will likely be needed for axisymmetric open system power plants, but there are a number of candidates [6].

The hot ion component with the energy optimal for fusion applications is commonly sustained in such systems by high-power neutral beam injection (NBI). In turn, the electrons are heated by collisions with NBI-driven energetic ions. Electrons with their superior mobility carry most of the heat flux, which flows mainly along magnetic field lines and hits the end plates outside the magnetic mirrors. Because of the higher electron mobility, the electron temperature (T_e) is significantly lower than the mean energy of fast ions. The energy confinement time of fast ions in a plasma with relatively cold electrons is determined by the electron-ion Coulomb collisions (electron drag), $\tau_\mathrm{h} \propto T_e^{3/2}$. For this reason, the electron temperature is the main factor limiting the confinement time of fast ions and, thus, the power efficiency of a beam-driven fusion reactor based on a magnetic mirror.

Widely believed estimates based on classical (Spitzer) electron thermal conductivity to end walls show that the heat flux along the magnetic field is proportional to $T_e^{7/2}$ [7], which would prevent any thermonuclear power application of mirror traps due to a poor quality of energy confinement. This, together with many experiments that never demonstrated an electron temperature higher than 280 eV [8], led to a judgment that fusion reactors based on magnetic mirrors were not feasible. As a result, much of the research activity in this field was discontinued.

However, plasma self-organization in a region behind the magnetic mirrors can lead to significant suppression of the longitudinal electron heat flux [9]. More recent theoretical work [10] has shown that electrons can be decoupled from the end walls (thereby, eliminating electron thermal conductivity to end walls) by expanding the magnetic field from that at the mirrors by at least the square root of the ion to electron mass ratio. This prevents secondary electrons generated at the end wall from reaching and cooling the hot plasma; in addition, the vacuum must be maintained at a sufficiently high level to keep ionization of gas to a minimal level.

 © 2015 American Physical Society

Previous experiments on the gas dynamic trap (GDT) facility in the Budker Institute with NBI are consistent with this theory [11,12] and have achieved electron temperatures of 250 eV, which is a factor of 5 higher than that limited by Spitzer heat conductivity. The experiments described here are even more definitive: demonstrating that electron temperatures in a magnetic mirror can exceed those limited by Spitzer heat conductivity, not by just factors of a few, but by an order of magnitude—these results are sufficient to justify working on magnetic mirrors as a potential path to fusion energy. Experiments towards this task were performed using a new 0.7 MW electron cyclotron resonance heating (ECRH) system in addition to the standard 5 MW NBI heating.

A schematic of the experiment is shown in Fig. 1. The GDT is a large-scale axially symmetric magnetic-mirror device with a 7-m-long central cell and two expander cells at both ends. The design, the physics of plasma confinement, and the main goals of this device are described in [13]. The ratio of the maximum and minimum values of the magnetic field between mirrors (the on-axis mirror ratio) is 35. All plasma-facing collectors are placed sufficiently far from the magnetic mirrors so that plasma expansion before the end plates reduces the electron heat transfer to far below the Spitzer value.

The GDT plasma consists of two components with different mean energies. One is the bulk plasma serving as a target for NBI. Because of high collisionality, this component has an isotropic Maxwellian velocity distribution with a temperature of 100–200 eV, both for ions and electrons; therefore, it is confined in the gas-dynamic regime [14]. The other plasma component consists of fast ions with a mean energy about 10 keV resulting from collisional slowing-down of NBI-born particles. The confinement time of fast ions is determined by the electron "drag" force, which is less than the ion-ion angular scattering time in the GDT. As a result, fast ions have a strongly anisotropic distribution function with a relatively small angular spread. Movement of the fast ions between rare collisions is governed by conservation of energy and adiabatic invariants. As a result they follow magnetic field lines between two turning points where their density and pressure are highly peaked. This nonequilibrium

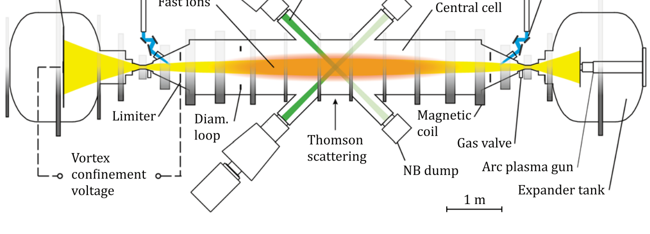

FIG. 1 (color online). Schematic of the GDT facility.

distribution, together with a high value of β, may cause microinstabilities, in particular, the loss cone instability [15]. However, such instabilities have never been observed at the GDT except for the Alfvén ion cyclotron instability, which does not lead to a noticeable loss of fast ions [16]. Absence of the loss cone instability of fast ions is attributed to the stabilizing effect of warm plasma ions [17], which have an isotropic distribution.

The main heating system consists of eight neutral-beam injectors providing 5 MW power incident on the plasma. Recently, the GDT has been upgraded with the addition of an ECRH system operating at 54.5 GHz with a total power 0.7 MW [18]. An attractive feature of this system is that the ECRH power is directly deposited into the electron component resulting in a total power comparable to that transmitted to electrons from the slowing-down of NBI-born fast ions (1 MW). Note that although ECRH techniques are well developed for toroidal fusion devices and small open traps, none of the existing schemes was suitable for the GDT conditions. Thus, we have developed a new ECRH scheme at the fundamental harmonic of the extraordinary plasma mode. We launch a microwave beam obliquely into the GDT plasma at an angle and position such that it is trapped inside a plasma column; then, after crossings of a plasma axis, the microwave beam reaches the cyclotron resonance surface and dissipates. More details may be found in [19].

The presently available power suppliers provide the magnetic field required for the ECRH at only one end of the machine. This would limit the experiment to one of two available heating beams. Experiments, with 0.4 MW ECRH at only one end, resulted in the on-axis electron temperature of 400–450 eV [20]. In this Letter, we report experiments for which we adopt another strategy. The magnetic field is reshaped such that it is increased in both ECRH regions, located near the trap ends, and is lowered everywhere else. This allows exploiting both available microwave beams and boosting the injected ECRH power to 0.7 MW. We also have the ability to tune the magnetic field inside the ECRH region. However, the magnetic field in the rest of the GDT is decreased (e.g., from 0.35 to 0.27 T in the central solenoid and proportionally in the mirrors), which results in some degradation of plasma confinement properties. In particular, without ECRH, the on-axis electron temperature is only 120–180 eV depending on a plasma density, while for the standard magnetic field configuration, this temperature is 250 eV with a plasma density of 2×10^{19} m^{-3} [12,21].

Another issue is the MHD stability of the bulk plasma, for which the current configuration of the GDT is inherently unstable. To suppress the anomalous transverse transport caused mainly by excitation of flute MHD modes, we use a novel technique which we call "vortex confinement" [22]. Strictly speaking, this method is not meant to suppress MHD modes, but rather to saturate them at a relatively low level by the differential rotation of outer plasma layers induced by an externally applied radial electric field. This produces a vortexlike structure with essentially closed flux lines. In the GDT, the vortex confinement technique is realized by applying a biasing potential between the ring-shaped radial plasma limiters and the central sections of plasma-facing end plates. The vortex confinement results in a stable confinement of hot plasma in the central core region, which appears to be unaffected by peripheral convection. The main conclusion based on the theoretical analysis [22] and experimental results [12] is that the transverse power losses can be limited to the level of 10%–15% of the longitudinal (gas-dynamic) losses.

Implementation of the vortex confinement in the GDT allowed achieving a record value, for axisymmetric traps, of $\beta \approx 0.6$ [12,21]. To provide an optimal confinement, the biasing potential should be close to the electron temperature. This condition is easily violated during the fast rise of the electron temperature in ECRH experiments. Thus, to stabilize plasma, we need to apply additional voltage to the plasma periphery during the ECRH phase.

The experiment is performed in a deuterium plasma. A typical discharge is presented in Fig. 2. The discharge is initiated by a plasma gun that injects a primary plasma along the axis from 0.5 to 4.5 ms. Plasma heating starts at 3.7 ms with 5 MW NBI, then 2.4 ms later, the additional 0.7 MW ECRH is switched on. The total discharge duration is about 9 ms while the ECRH phase lasts 2.5 ms. From a diamagnetic signal (c), one can see that, without the additional bias voltage to the plasma limiter, ECRH may result in a rapid degradation of the plasma confinement—the steady heating switches on a full-scale instability leading to the loss of the entire plasma. The discharge is stabilized by increasing the limiter potential during the ECRH phase, but, even with this, the instability is not entirely suppressed, as seen in the time resolved measurements of the on-axis electron temperature (a) and the magnetic fluctuations (b). Though the diamagnetic signal that measures the integrated plasma pressure is maintained at the same level or even grows until the NBI is switched off, the peaked temperature profile cannot be supported during the whole ECRH pulse due to the triggering of a low-frequency instability visible in signals from magnetic probes. More careful analysis of magnetic data reveals a $m = 1$ azimuthal flute mode at a frequency of about 10 kHz that develops when the electron temperature exceeds the limiter potential. Nevertheless, the duration of stable microwave heating has been increased up to 0.6 ms resulting in the record electron temperature registered at GDT to date. Even though the MHD activity is still present, it no longer leads to the dramatic loss of the entire plasma and tends to become less destructive with the increase of the limiter potential.

Electron temperature and density are measured in the central plane by Thomson scattering diagnostics based on a

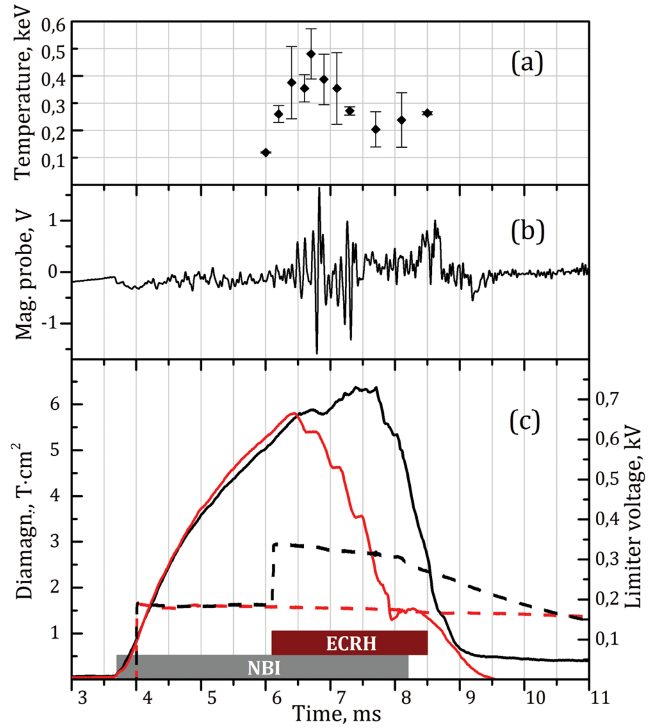

FIG. 2 (color online). Evolution of (a) the on-axis electron temperature during the ECR heating measured using the Thomson scattering system; (b) the signal from a radial magnetic field probe indicated a low-frequency flute instability; (c) the diamagnetic signal mostly contributed by the hot ion pressure (solid line) and the bias potential used for plasma stabilization (dashed line) during combined 5 MW NBI and 0.7 MW ECRH discharges with (black lines) and without (red lines online) additional voltage ($\approx$ 150 V) applied to the limiter at the GDT facility. Note the flute instability that develops at 6.5 ms far before the plasma decay associated to NBI switching off at 8 ms.

1 μm laser. In Fig. 3, we present Thomson scattering data for the on-axis electron temperature. This plot is obtained by averaging over a continuous series of consecutive shots, demonstrating a good shot-to-shot reproducibility. The scattered spectrum proves that the electron velocity distribution remains Maxwellian with the average electron temperature of 660 ± 50 eV. It should be noted that, in a few shots, the measured electron temperature exceeds 900 eV. The plasma density is about 0.7×10^{19} m^{-3} for all shots. These values were obtained in the most favorable ECRH conditions found experimentally. In total, there are more than 200 successful discharges with the on-axis electron temperature above 300 eV that have been registered during the reported campaign; their distribution over measured temperatures is presented in Table I.

In Fig. 4, we show typical radial profiles of the electron temperature and plasma density measured in the central cell without ECRH and at 0.6 ms after ECRH start up. The peaked temperature profile with additional heating suggests that the microwave power is deposited inside a central

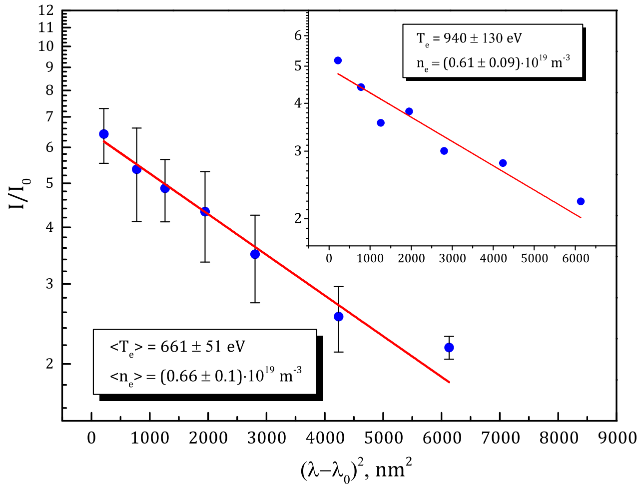

FIG. 3 (color online). Electron energy spectrum measured by Thomson scattering on the axis and averaged over 7 consecutive shots. Fit of these data suggests a Maxwellian electron distribution function (represented by a straight line in the semilog plot) with an electron temperature of 660 ± 50 eV and a density $(0.66 \pm 0.10) \times 10^{19}$ m^{-3}. The same data for one of the shots with an electron temperature above 900 eV are shown in the inset.

region with a characteristic radius ~5 cm with little deposition in the peripheral plasma. This contradicts both the initial theoretical proposal [19] and the low-power experiment [20] in which the microwave power is spread through the whole plasma cross section rather than focused in a narrow region around the machine axis. This contradiction may be explained by a combination of two factors. First, for the new plasma configuration, the ray tracing, indeed, predicts that ECRH power deposition has a gap outside of the core plasma: 30% of total injected power is deposited in the core plasma with $r < 5$ cm, 40% of power goes to the peripheral plasma with $r > 20$ cm, and the rest of the power is not absorbed. Another reason for the temperature peaking is a reduced magnetic field in the central cell that results in poor confinement at the plasma periphery as compared to the standard configuration.

It should be stressed that, in spite of reduced confining properties of the new magnetic configuration, the power balance indicates that the core plasma is trapped in the gas-dynamic regime [14]. Indeed, assuming that all the electron energy is lost due to plasma streaming with the ion-acoustic velocity $v_s \propto T_e^{1/2}$ along the magnetic field lines, one can estimate the power density required to support a stationary discharge with a given electron temperature as $p \propto v_s T_e \propto T_e^{3/2}$. Previously, this scaling has been proven experimentally for discharges without ECRH [13]. Then, we can compare two discharges, before and during the stable ECRH stage, assuming that only the temperature and power are varying,

$$T_e^{\mathrm{ECRH}}/T_e^{\mathrm{NBI}} = (p^{\mathrm{ECRH}}/p^{\mathrm{NBI}})^{2/3},$$

TABLE I. Distribution of high-temperature shots in experiments with reduced magnetic field and 700 kW ECRH.

On-axis electron temperature (eV)	Total number of shots
300–500	165
500–700	43
700–900	8
900–1100	3

where $p^{\mathrm{NBI}} \approx 40$ kW is the NBI power deposited into electrons without ECRH, and $p^{\mathrm{ECRH}} \approx 200$ kW is the total ECRH and NBI power after ECRH is switched on. Both powers are calculated by ray tracing and fast ion slowing-down codes for the core plasma region within $r < 7$ cm (for the plasma profiles shown in Fig. 4). This estimate gives about a threefold increase in the electron temperature that is in agreement with our measurements. Note that the classical heat flux for electrons with a temperature of 500 eV corresponds to power losses of GW level.

Summarizing our experience in ECRH supported discharges at the GDT facility, we may conclude that reaching a high electron temperature in an open trap with a dense plasma results in the less efficient vortex stabilization. This problem is manageable, but, eventually, we will have to find some compromise between the high temperature and MHD stability in practical applications. In the present Letter, we aim to demonstrate the highest possible (in a quasistationary discharge) electron temperature with available resources. To make it possible, we focus the

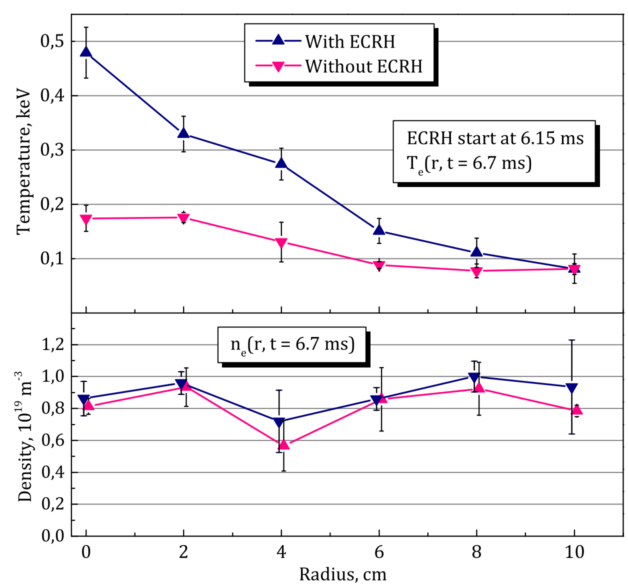

FIG. 4 (color online). Radial profiles of the electron temperature and density at the trap center. Thomson scattering diagnostics resolves one radial point per shot; thus, these profiles were obtained over a series of identical shots. To improve reproducibility, we use a scenario with a peak electron temperature slightly lower than that indicated in Fig. 3.

microwave power deposition on the plasma axis reaching a very high local power density (up to 20 kW/cm^2 compared to 0.1–0.3 kW/cm^2 typical of purely NBI heating). Moreover, ray-tracing calculations reveal a positive feedback: a temperature increase results in better absorption and, consequently, in stronger peaking of the temperature profile. We find that our theoretical understanding of resonant plasma heating has been proven experimentally; thus, the proposed novel ECRH scheme works quite robustly.

The measured increase of electron temperature to nearly 1 keV along with results of previous GDT experiments, which demonstrated high-density plasma confinement with $\beta \approx 60\%$, provide a firm basis for extrapolating the gas-dynamic-trap concept to fusion relevant applications. These electron temperatures are adequate for a neutron source that needs $T_e \sim 700$ eV to test and develop fusion materials, or to initiate work on subcritical fission reactors and nuclear waste processing based on a fusion driven burning of minor actinides [2]. In addition, these results encourage expectations that the higher temperatures needed for fusion power are possible.

The authors are grateful to M. Thumm for his advice concerning physical and technical aspects of ECR heating, to A. Molvik for his great encouragement and help in preparation of this Letter, also to A. Anikeev, A. Arzhannikov, A. Ivanov, V. Malygin, T. Simonen, O. Smolyakova, V. Orlov, D. Ryutov, and K. Zaytsev for their support and assistance. We thank all the GDT team who participated in the experiment. The work is supported by the Russian Scientific Foundation (Project No. 14-12-01007).

*p.a.bagryansky@inp.nsk.su
†ags@appl.sci-nnov.ru

[1] F. H. Coengsen, T. A. Casper, D. L. Correll, C. C. Damm, A. H. Futch, B. GLogan, A. W. Molvik, and C. E. Walter, J. Fusion Energy **8**, 237 (1989).
[2] P. A. Bagryansky, A. A. Ivanov, E. P. Kruglyakov, A. M. Kudryavtsev, Yu. A. Tsidulko, A. V. Andriyash, A. L. Lukin, and Yu. N. Zouev, Fusion Eng. Des. **70**, 13 (2004).
[3] L. J. Perkins, B. G. Logan, R. B. Campbell, R. S. Devoto, D. T. Blackfield, and B. H. Johnson, Fusion Technol. **8**, 685 (1985).
[4] A. Beklemishev *et al.*, Fusion Sci. Technol. **63**, 46 (2013).
[5] R. F. Post *et al.*, Fusion Sci. Technol. **47**, 49 (2005).
[6] D. D. Ryutov, H. L. Berk, B. I. Cohen, A. W. Molvik, and T. C. Simonen, Phys. Plasmas **18**, 092301 (2011).
[7] L. Spitzer, Jr., *Physics of Fully Ionized Gases*, 2nd ed. (Interscience, New York, 1962).
[8] For example, $T_e \approx 60$ eV at 2XIIB experiment, see B. G. Logan *et al.*, Phys. Rev. Lett. **37**, 1468 (1976); $\boldsymbol{T_e} \approx 40$ **eV** at Gamma 10, see M. Yoshikawa *et al.*, Rev. Sci. Instrum. **85**, 11D801 (2014); and the best published result $\boldsymbol{T_e} \approx$ 280 **eV** achieved on TMX-U, see T. C. Simonen and R. Horton, Nucl. Fusion **29**, 1373 (1989).
[9] I. K. Konkashbaev, I. S. Landman, and F. R. Ulinich, Zh. Exp. Teor. Fiz. **74**, 956 (1978).[J. Exp. Theor. Phys. **47**, 501 (1978)].
[10] D. D. Ryutov, Fusion Sci. Technol. **47**, 148 (2005).
[11] A. V. Anikeev, P. A. Bagryansky, G. I. Kuznetsov, and N. V. Stupishin, Plasma Phys. Rep. **25**, 775 (1999).
[12] P. A. Bagryansky, A. V. Anikeev, A. D. Beklemishev, A. S. Donin, A. A. Ivanov, M. S. Korzhavina, and K. V. Zaytsev, Fusion Sci. Technol. **59**, 31 (2011).
[13] A. A. Ivanov and V. V. Prikhodko, Plasma Phys. Controlled Fusion **55**, 063001 (2013).
[14] The term, gas dynamic, makes an analogy between gas flowing out of a can with a small pinhole with isotropic, collisional plasma flowing out of a magnetic flux tube constricted by a high mirror ratio, see e.g., V. V. Mirnov and D. D. Ryutov, Sov. Tech. Phys. Lett. **5**, 279 (1979).
[15] M. S. Ioffe, B. I. Kanaev, V. P. Pastukhov, and E. E. Yushmanov, Zh. Exp. Teor. Fiz. **67**, 2145 (1975) [Sov. Phys. JETP **40**, 1064 (1975)].
[16] K. V. Zaytsev *et al.*, Phys. Scr. T **T161**, 014004 (2014).
[17] B. G. Logan *et al.*, Phys. Rev. Lett. **37**, 1468 (1976).
[18] P. A. Bagryansky *et al.*, Fusion Sci. Technol. **63**, 40 (2013).
[19] A. G. Shalashov, E. D. Gospodchikov, O. B. Smolyakova, P. A. Bagryansky, V. I. Malygin, and M. Thumm, Phys. Plasmas **19**, 052503 (2012).
[20] P. A. Bagryansky, Yu. V. Kovalenko, V. Ya. Savkin, A. L. Solomakhin, and D. V. Yakovlev, Nucl. Fusion **54**, 082001 (2014).
[21] T. C. Simonen, A. Anikeev, P. Bagryansky, A. Beklemishev, A. Ivanov, A. Lizunov, V. V. Maximov, V. Prikhodko, and Yu. Tsidulko, J. Fusion Energy **29**, 558 (2010).
[22] A. D. Beklemishev, P. A. Bagryansky, M. S. Chaschin, and E. I. Soldatkina, Fusion Sci. Technol. **57**, 351 (2010).